Published in final edited form as:
Nat Methods. 2020 August 01; 17(8): 789–791. doi:10.1038/s41592-020-0869-x.

Up to 100-fold speedup and multiplexing in optimized DNA-PAINT

Sebastian Strauss[1,2], **Ralf Jungmann**[1,2]

[1]Faculty of Physics and Center for Nanoscience, Ludwig Maximilian University, Munich, Germany

[2]Max Planck Institute of Biochemistry, Martinsried, Germany

Abstract

DNA-PAINT's imaging speed has recently been significantly enhanced by optimized sequence design and buffer conditions. However, this implementation has not reached an ultimate speed-limit and importantly is only applicable to imaging single targets. To further improve acquisition speed, we here introduce concatenated, periodic DNA sequence motifs, yielding up to 100-fold faster sampling compared to traditional DNA-PAINT. We extend this approach to six orthogonal sequence motifs, now enabling speed-optimized multiplexed imaging.

Super-resolution imaging has enabled the visualization of biological structures below the classical diffraction limit of light[1–3]. DNA-PAINT is an easy to implement super-resolution technique providing better than 5 nm spatial resolution, as previously demonstrated on DNA nanostructures[4]. Furthermore, we have recently combined DNA-PAINT with small labeling probes to translate this high spatial resolution to cellular imaging on the level of single proteins[5, 6]. In addition, DNA-barcoded labeling probes in combination with sequential readout enables spectrally-unlimited multiplexing in Exchange-PAINT[7]. However, in practice, the biological applicability of DNA-PAINT is restricted due to rather slow imaging, often resulting in acquisition times of up to hours[8]. In fact, the imaging speed is limited by the intrinsic hybridization kinetics of the respective docking and imager strand sequence pair. Recently, this issue has been addressed by rational sequence design[9] and careful buffer optimization resulting in an order of magnitude faster DNA-PAINT image acquisition[10]. Further improvement has been achieved by preloading DNA-PAINT imager strands with Argonaute proteins[11]. While these advancements in image acquisition speed have paved the way towards high-throughput studies using DNA-PAINT, a ten-fold improvement might not

Correspondence to: Ralf Jungmann.

Correspondence should be addressed to R.J. (jungmann@biochem.mpg.de).

Author contributions

S.S. conceived and performed experiments, analyzed data, and contributed to the writing of the manuscript. R.J. conceived and supervised the study, interpreted data, and wrote the manuscript. All authors reviewed and approved the manuscript.

Competing interests

The authors declare no competing interests.

Reporting Summary. Further information on research design is available in the Nature Research Reporting Summary linked to this article.

Europe PMC Funders Author Manuscripts

be the ultimate speed limit. Furthermore, while the sequence optimization alone yielded a respectable 5-fold speed increase for the best-performing sequence, it lacks multiplexing capability, as orthogonal sequences yielding similar hybridization properties have not been available.

Here, we introduce a novel concept to further increase imaging speed in DNA-PAINT, by using the fact that the frequency of imagers binding to their docking strands scales linearly with the number of available binding sites, a fact that has been central to quantitative imaging in qPAINT[12]. An intuitive way to achieve multiple docking sequences per target would be to simply change a single complementary sequence (Fig. 1a) to a concatenated version (e.g. five repeats, see top of Fig. 1b). However, while this seems logical, it comes at the disadvantage of also increasing the length of the docking strand, e.g. from 7 nt for one to 35 nt for five concatenated sites. This might not only lead to a potential reduction in spatial resolution, but possibly to increased non-specific binding to cellular components. To address both issues, we here opted for a more compact sequence design featuring a repetitive sequence motif, e.g. $(TCC)_n$ (Fig. 1a), which can be concatenated to provide overlapping binding sites (Fig. 1b, bottom). This allows us to theoretically design five docking site repeats, yet only increasing the strand length to 19 nt, rather than 35 nt. To test our approach, we designed two DNA origami 20-nm-grids[13] carrying 1x and 5x versions of our overlapping sequence design (called R1) targeted with Cy3B-labeled imager strands. DNA-PAINT imaging of both structures showed significantly improved sampling for the 5x versions and subsequent qPAINT analysis yielded an approximate 5-fold increase in the mean number of binding events (99 vs. 515) for origami structures carrying 5xR1 sequences (Fig. 1c and d, Extended Data Figure 1). We furthermore quantitatively assessed the number of detected binding events for up to 10 repeats on single binding sites on DNA origami, resulting in a linear increase in binding events with the number of repeats (Fig. 1e and Supplementary Figure 1).

We then turned our attention to introduce multiplexing capabilities to speed-optimized DNA-PAINT by designing five additional orthogonal sequence motifs, which could again be concatenated to form overlapping binding sites (Fig. 2a). These were either based on a motif containing three bases – R2 $(ACC)_n$, R5 $(CTT)_n$, R6 $(AAC)_n$ – or 2-bases – R3 $(CT)_n$, R4 $(AC)_n$ – while maintaining a two-letter-code sequence (i.e. AC or TC only) to avoid transient hairpin formation of the docking site[9, 10]. We assayed their hybridization kinetics using DNA origami with single docking sites (Extended Data Figures 2–3, Supplementary Figures 2–3). Like the R1 sequence described above, concatenation of R2 to R6 sequences also revealed a linear increase in binding frequency. Using six 20-nm-grid structures carrying R1–R6 docking sites, we could show that imager strands bind specifically to their corresponding docking sites only, thus providing quantitative proof of their respective orthogonality (Extended Data Figure 4, Supplementary Figure 4). In order to benchmark the achievable Exchange-PAINT imaging speed, we used the same origami structures and were able to clearly resolve 20-nm distances with sufficient sampling after 5 min for each round, resulting in a total raw image acquisition time of just 30 min for the 6-plex super-resolution experiment (Fig. 2b and c, Extended Data Figure 5). We note that we did not observe a considerable effect of photo-induced depletion of docking sites[14] due to shorter overall

binding times of the sequences and the use of and oxygen scavenger and triplet state quencher system[15] (PCA, PCD, and Trolox, see Online Methods).

Despite the extended length of the concatenated docking strands, we were furthermore able to maintain DNA-PAINT's sub-5-nm spatial resolution capability, substantiated by imaging 5-nm features on 'MPI' logos designed on DNA origami (Fig. 2d and Extended Data Figure 6). Due to the relatively low imager concentration of 200 pM, we achieved a high signal-to-noise ratio, enabling 5-nm resolution with a camera integration time of only 100 ms (compared to 350 ms used in previous works[4]). Next, we applied our new approach to cellular imaging. We site-specifically coupled the 5xR1 sequence to a GFP nanobody[16, 17] and visualized the nuclear pore complex protein Nup96 in EGFP-Nup96 U2OS cells[18, 19]. We achieved highly specific and efficient labeling at sub-10-nm spatial resolution (Fig. 2e and Extended Data Figure 7). We furthermore demonstrated two-plex Exchange-PAINT imaging using a combination of primary and secondary antibodies for tubulin and vimentin (Extended Data Figure 8) showing specific labeling of cytoskeletal structures.

Finally, we performed 4-plex Exchange-PAINT using four of the new sequences to demonstrate cellular imaging with single-protein resolution by targeting the Receptor Tyrosine Kinases EGFR, Her2, ErbB3 and c-Met. To accomplish this, we used a commercially-available double knock-in cell line (SKOV-3 expressing GFP-Her2 and tagRFP-EGFR) and DNA-conjugated nanobodies against both fluorescent proteins[20]. In addition, we employed a combination of primary antibodies and DNA-conjugated secondary nanobodies[17] to label c-Met and ErbB3 in these cells (Figure 2f and Extended Data Figure 9). We obtained single-protein resolution with calculated localization precisions[21] of approx. 5 nm (Supplementary Table 10) for all four receptors and visualized homo- and heterodimerization of these RTKs with measured distances between 16–22 nm (Fig. 2g).

In conclusion, we have introduced a new concept to design docking sites with tunable hybridization kinetics and demonstrated up to 100-fold faster imaging compared to classical DNA-PAINT. At the same time, we introduced up to 6-plex Exchange-PAINT imaging using speed-optimized docking sites. Besides faster DNA-PAINT, the new sequences enable imaging at lower imager concentration, leading to reduced background and thus increased signal-to-noise. We note that the considerable increase in sampling frequency will potentially prove crucial in biological applications in tissues or imaging of nuclear targets further away from the coverslip where high signal-to-noise is essential. A further promising application is to employ changes of kinetic hybridization properties for multiplexing using kinetic barcoding as previously reported[22]. For instance, the R3 sequence motif provides clearly distinguishable bright (τ_B) and dark times (τ_D), thus enabling efficient kinetic barcoding e.g. on the level of single target proteins, which was thus far not achievable[22] (Extended Data Figure 10). Finally, the further improved sampling frequency compared to traditional DNA-PAINT could now enable single-protein-sensitive, high-resolution studies of a multitude of surface receptor proteins and other biomedical applications with sample statistics thus far out of reach.

Methods

Materials

Unmodified DNA oligonucleotides were purchased from MWG Eurofins and Metabion. C3-azide, Cy3B and ATTO 655 modified DNA oligonucleotides were ordered from Metabion and MWG Eurofins. M13mp18 scaffold was obtained from Tilibit. Magnesium 1 M (cat: AM9530G), sodium chloride 5 M (cat: AM9759), ultrapure water (cat: 10977-035), Tris 1 M, pH 8 (cat: AM9855G), EDTA 0.5 M, pH 8.0 (cat: AM9260G) and 10×PBS (cat: 70011051) was purchased from Thermo Fisher Scientific. Bovine serum albumin (cat: A4503-10G) was ordered from Sigma-Aldrich. Triton X-100 (cat: 6683.1), Sodium borohydride > 97 % (cat: 4051.1), ammonium chloride (cat: K298.1), and potassium chloride (cat: 6781.1) was purchased from Carl Roth. Sodium hydroxide (cat: 31627.290) was purchased from VWR. Paraformaldehyde (cat: 15710) and glutaraldehyde (cat: 16220) were obtained from Electron Microscopy Sciences. Tween 20 (cat: P9416-50ML), glycerol (cat: 65516-500ml), methanol (cat: 32213-2.5L), protocatechuate 3,4-dioxygenase pseudomonas (PCD) (cat: P8279), 3,4-dihydroxybenzoic acid (PCA) (cat: 37580-25G-F) and (+−)-6-hydroxy-2,5,7,8- tetra-methylchromane-2-carboxylic acid (Trolox) (cat: 238813-5 G) were ordered from Sigma Aldrich. Streptavidin (cat: S-888) was purchased from Thermo Fisher. BSA-Biotin (cat: A8549) was obtained from Sigma-Aldrich. Coverslips (cat: 0107032) and glass slides (cat: 10756991) were purchased from Marienfeld and Thermo Fisher Scientific. Double-sided tape (cat: 665D) was ordered from Scotch. Two component silica twinsil speed 22 (cat. 1300 1002) was purchased from Picodent. Fetal Bovine Serum (FBS) (cat: 10500-064), 1× Phosphate Buffered Saline (PBS) pH 7.2 (cat: 20012-019), 0.05 % Trypsin–EDTA (cat: 25300-054) and were purchased from Thermo Fisher Scientific. 90 nm diameter Gold Nanoparticles (cat: G-90-100) were ordered from cytodiagnostics.

Buffers

The following buffers were used for sample preparation and imaging

- Buffer A: 10 mM Tris pH 8, 100 mM NaCl, 0.05 % Tween 20
- Buffer B: 10 mM $MgCl_2$, 5 mM Tris-HCl pH 8, 1 mM EDTA, 0.05 % Tween 20, pH 8
- Buffer C (Imaging buffer): 1× PBS, 1mM EDTA, 500 mM NaCl, pH 7.4. Optionally supplemented with: 1× Trolox, 1× PCA and 1× PCD
- Blocking buffer: 1× PBS pH 7.4, 1 mM EDTA, 3% BSA, 0.02% Tween-20.

Trolox, PCA and PCD

100× Trolox: 100 mg Trolox, 430 µl 100 % Methanol, 345 µl 1M NaOH in 3.2 ml H_2O. 40× PCA: 154 mg PCA, 10 ml water and NaOH were mixed and pH was adjusted 9.0. 100× PCD: 9.3 mg PCD, 13.3 ml of buffer (100 mM Tris-HCl pH 8, 50 mM KCl, 1 mM EDTA, 50 % Glycerol).

DNA origami self-assembly

All DNA origami structures were designed with the Picasso design tool[4]. Self-assembly of DNA origami was accomplished in a one-pot reaction mix with 40 µl total volume, consisting of 10 nM scaffold strand (sequence see Supplementary Spreadsheet 1), 100 nM folding staples (Supplementary Spreadsheet 2–4), 500 nM biotinylated staples (Supplementary Table 3), and 1 µM of staple strands with docking site extensions (for respective sequences see Supplementary Table 4 and 5 andSupplementary Data 2–4) in folding buffer (5 mM Tris pH 8, 1 mM EDTA 12.5 mM $MgCl_2$). The reaction mix was then subjected to a thermal annealing ramp using a thermocycler. The reaction mix was first incubated at 80 °C for 5 min, then cooled down using a temperature gradient from 60 to 4 °C in steps of 1 °C per 3.21 min and finally held at 4 °C.

DNA origami purification

DNA origami structures were purified via ultrafiltration using Amicon Ultra Centrifugal Filters with a 50 kDa MWCO (Merck Millipore, UFC505096) as previously described[23]. In brief, folded origami was filled up to 500 µl with FoB5 buffer (5 mM Tris, 1 mM EDTA, 5 mM NaCl, 5 mM MgCl2, pH 8) and spun for 6 min at 5000 g. This process was repeated twice. Purified DNA origami structures were recovered into a new tube by centrifugation for 5 min at 5000 g.

DNA origami sample preparation

For sample preparation, a piece of coverslip and a glass slide were sandwiched together by two strips of double-sided tape to form a flow chamber with inner volume of ~20 µl. First, 20 µl of biotin labeled bovine albumin (1 mg/ml, dissolved in buffer A) was flushed into the chamber and incubated for 2 min. The chamber was then washed with 40 µl of buffer A. A volume of 20 µl of streptavidin (0.1 mg/ml, dissolved in buffer A) was then flushed through the chamber and allowed to bind for 2 min. After washing with 20 µl of buffer A and subsequently with 20 µl of buffer B, 20 µl of biotin labeled DNA structures (~200 pM) in buffer B were flushed into the chamber and incubated for 2 min. The chamber was washed with 40 µl of buffer B. Finally, 20 µl of the imager solution in imaging buffer (see Supplementary Table 8) was flushed into the chamber, which was subsequently sealed with two component silica before imaging. For multiplexing experiments a bottomless 6 channel slide (ibidi, cat: 80608) was attached to a coverslip. The same sample preparation was performed as described above with adjusted volumes of 120 µl for each washing and incubation step. In between imaging rounds the sample was washed 4–5 times with 120 µl PBS until no residual signal from the previous imager solution was detected (total washing time of approx. 3–5 min). Then, the next imager solution was introduced.

Antibody-DNA conjugation

Antibodies were conjugated to DNA-PAINT docking sites (see Supplementary Table 7) via DBCO-sulfo-NHS ester chemistry as previously reported[4]. In brief, antibodies were reacted with 20-fold excess of a bifunctional DBCO-sulfo-NHS ester (Jena Biosciences, cat: CLK-A124-10). Unreacted linker was removed using Zeba Spin Desalting columns (0.5 ml, 40k MWCO, Thermo Fisher Scientific, cat: 89882). Azide-DNA was added to the DBCO-

antibodies with a 10-fold molar excess and reacted overnight at 4°C. Afterwards, buffer was exchange to PBS using Amicon centrifugal filters (100k MWCO).

Nanobody-DNA conjugation

Nanobodies against GFP, tagFP, rabbit and mouse IgG were purchased from Nanotag with a single ectopic cysteine at the C-terminus for site specific and quantitative conjugation. The conjugation to DNA-PAINT docking sites (see Supplementary Table 7) was performed similar as described previously[20]. First, buffer was exchanged to 1× PBS + 5 mM EDTA, pH 7.0 using Amicon centrifugal filters (10k MWCO) and free cysteines were reacted with 20-fold molar excess of bifunctional maleimide-DBCO linker (Sigma Aldrich, cat: 760668) for 2-3 hours on ice. Unreacted linker was removed by buffer exchange to PBS using Amicon centrifugal filters. Azide-functionalized DNA was added with 5-10 molar excess to the DBCO-nanobody and reacted overnight at 4°C. Unconjugated nanobody and free azide-DNA was removed by anion exchange using an ÄKTA Pure liquid chromatography system equipped with a Resource Q 1 ml column.

Cell culture

U-2 OS-CRISPR-Nup96-mEGFP (gift from Ries and Ellenberg lab) and SKOV3 GFP-Her2 RFP-tagEGFR cells (purchased from Sigma Aldrich, cat: CLL1143-1VL) were cultured in McCoy's 5A medium (Thermo Fisher Scientific, cat: 16600082) supplemented with 10% fetal bovine serum. For imaging, cells were seeded 1-2 days prior to fixation into Glass-bottomed 8-well μ-slides (ibidi, cat: 80827).

Cell fixation

All fixatives were pre-heated to 37°C before adding to the cells.

Microtubules and vimentin

U-2 OS-CRISPR-Nup96-mEGFP cells were first pre-extracted with 0.3 % glutaraldehyde and 0.25 % Triton X-100 for 90 s, followed by fixation with 3 % glutaraldehyde for 10 min. Afterwards, samples were rinsed twice with PBS and free aldehyde groups were reduced with 0.1 % $NaBH_4$ for 5 min. After rinsing four times with PBS, cells were blocked and permeabilized in blocking buffer with 0.25 % Triton X-100 for 2 h. Primary antibodies against anti-vimentin and anti-α-tubulin were incubated overnight at 4°C. After washing unbound primary antibodies for four times with PBS, secondary antibodies conjugated to DNA-PAINT docking sites were diluted in blocking buffer and incubated with the cells for 1 hour at room temperature. Finally, unbound antibodies were removed by washing three times with PBS for 5 min.

Nup96-EGFP imaging

U-2 OS-CRISPR-Nup96-mEGFP cells were fixed with 2.4% PFA in PBS for 30 min at room temperature. After fixation cells were washed three times with PBS and incubated with 0.1 M NH_4Cl in PBS for 5 min. Then, cells were permeabilized with 0.25% Triton-X-100 for 5 min and afterwards blocked in blocking buffer for 1 hour. Anti-GFP nanobodies were incubated at a concentration of appr. 50 nM in blocking buffer supplemented with 0.05

mg/ml sheared salmon sperm DNA overnight at 4°C. Unbound nanobodies were removed by washing three times with PBS for 5 min.

Receptor tyrosine kinases

SKOV3 GFP-Her2 tagRFP-EGFR cells were fixed with 4% PFA. After fixation, cells were washed three times with PBS and incubated with 0.1 M NH_4Cl in PBS for 5 min. Then, cells were permeabilized with 0.25% Triton-X-100 for 15 min and afterwards blocked in blocking buffer for 1 hour. Nanobodies and primary antibodies (see Supplementary Table 6) were diluted in blocking buffer supplemented with 0.05 mg/ml sheared salmon sperm DNA and incubated with the cells overnight at 4°C. Unbound nanobodies and antibodies were removed by washing three times with PBS for 5 min.

Microscope setup

Fluorescence imaging was carried out on an inverted microscope (Nikon Instruments, Eclipse Ti2) with the Perfect Focus System, applying an objective-type TIRF configuration equipped with an oil-immersion objective (Nikon Instruments, Apo SR TIRF 100×, NA 1.49, Oil). A 561 nm and 642 nm laser (MPB Communications Inc., 2 W, DPSS-system) were used for excitation. The laser beams were passed through cleanup filters (Chroma Technology, ZET561/10, ZET 640/10) and coupled into the microscope objective using a beam splitter (Chroma Technology, ZT561rdc, ZT640rdc). Fluorescence light was spectrally filtered with an emission filter (Chroma Technology, ET600/50m and ET700/75m) and imaged on a sCMOS camera (Andor, Zyla 4.2 Plus) without further magnification, resulting in an effective pixel size of 130 nm (after 2×2 binning). Images were acquired choosing a region of interest with the size of 512×512 pixels. More detailed imaging conditions for the respective experiments are shown in Supplementary Table 8.

Image analysis

Raw fluorescence data was subjected super-resolution reconstruction using the ‘Picasso’ software package[4] (Latest version available on https://github.com/jungmannlab/picasso). Drift correction was performed with a redundant cross-correlation and gold particles as fiducials. Gold particles were also used to align multiple rounds for Exchange-PAINT experiments. For quantification of binding kinetics, localizations were linked allowing a gap size of 3 frames and a maximum distance of 130 nm. Origami structures were automatically selected using Picasso’s ‘Pick similar’ function. Kinetic information of detected picks was extracted with the ‘save pick properties’ command. Further quantification such as histogram analysis and fitting were performed with Origin Pro (Version 2019b). Kinetic barcoding analysis (Extended Data Figure 10) was performed as previously described[22]. The data was segmented using the HDBSCAN clustering algorithm[24] with input parameter ‘Min_cluster size’ set to 10.

Europe PMC Funders Author Manuscripts

Europe PMC Funders Author Manuscripts

Extended Data

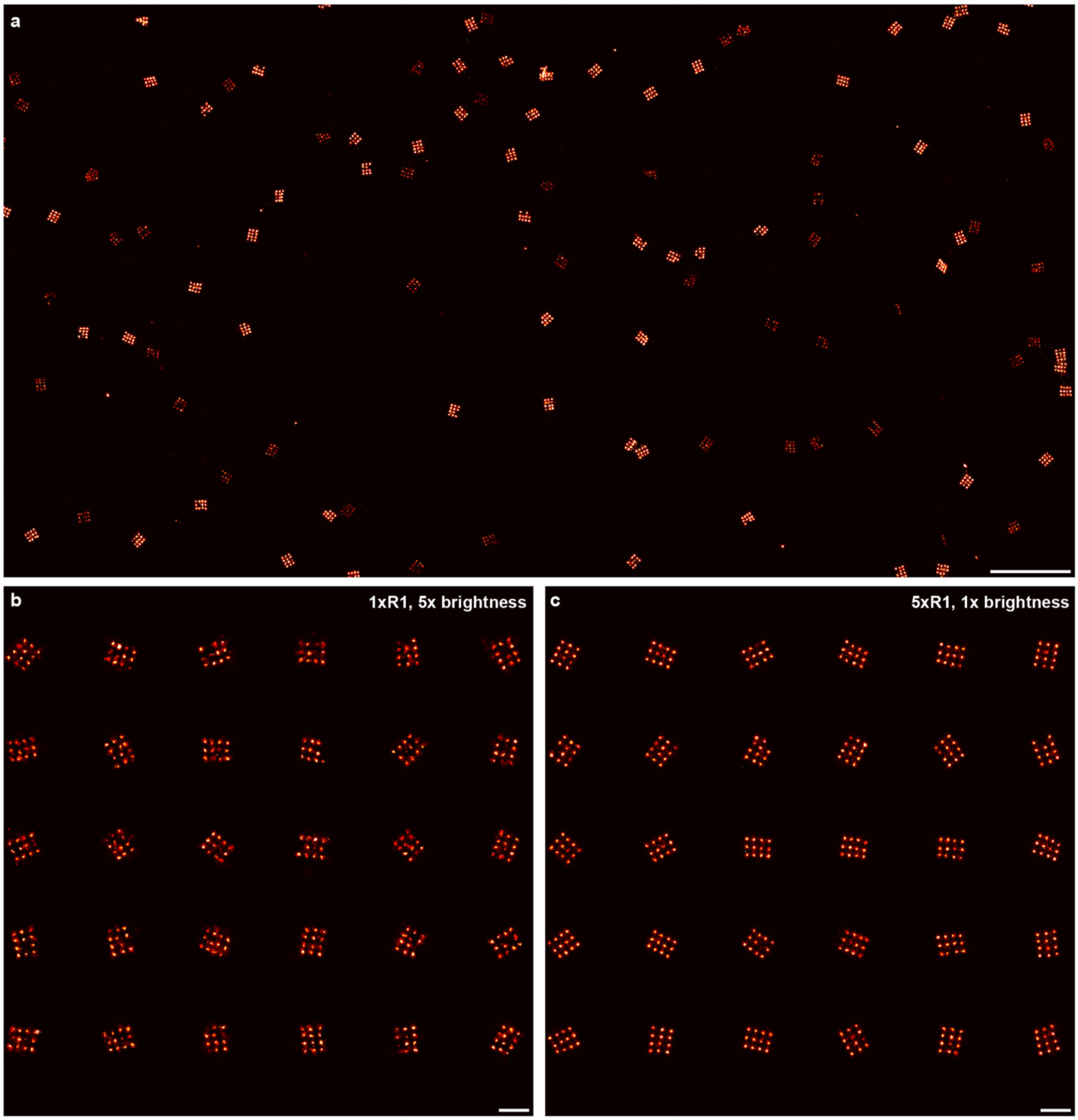

Extended Data Fig. 1.

Europe PMC Funders Author Manuscripts

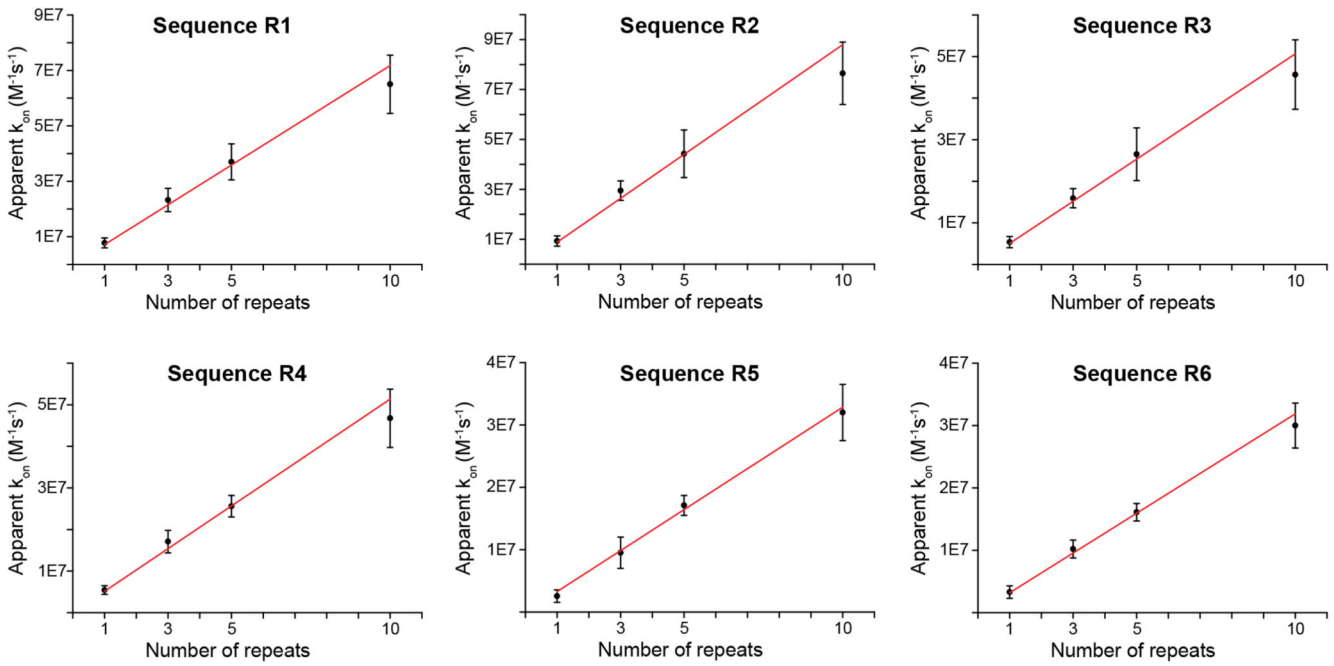

Extended Data Fig. 2.

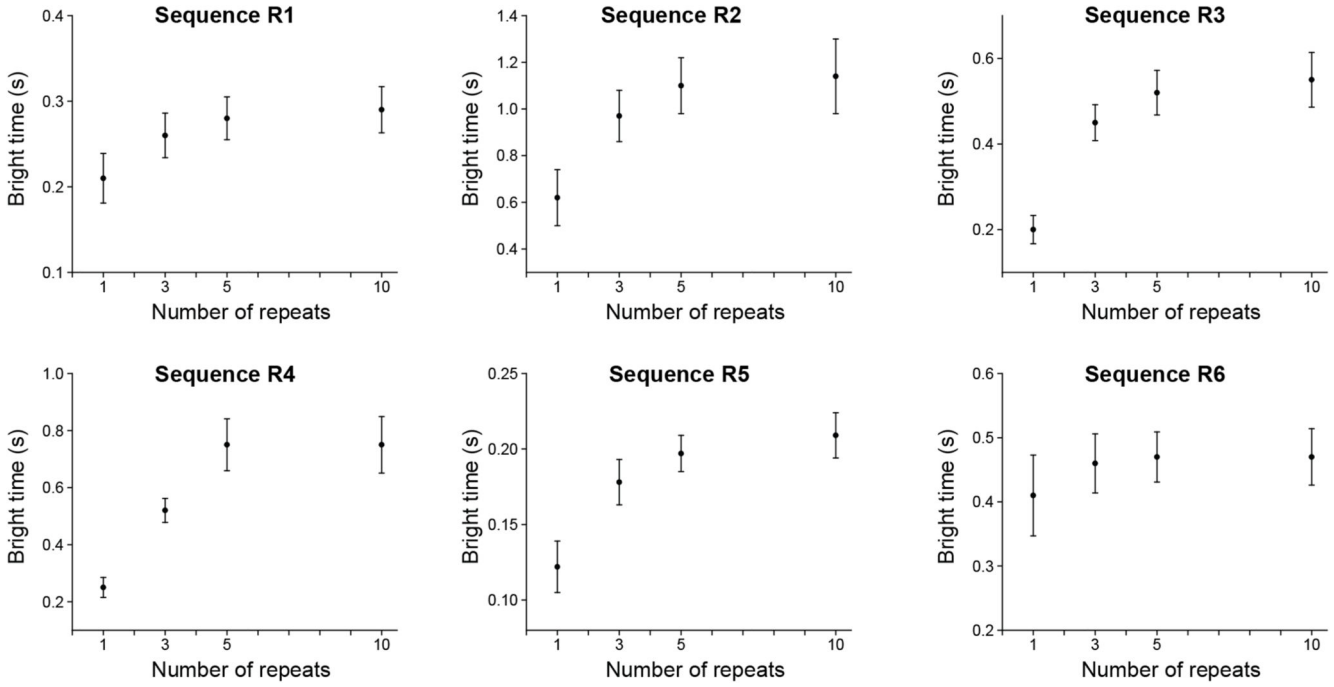

Extended Data Fig. 3.

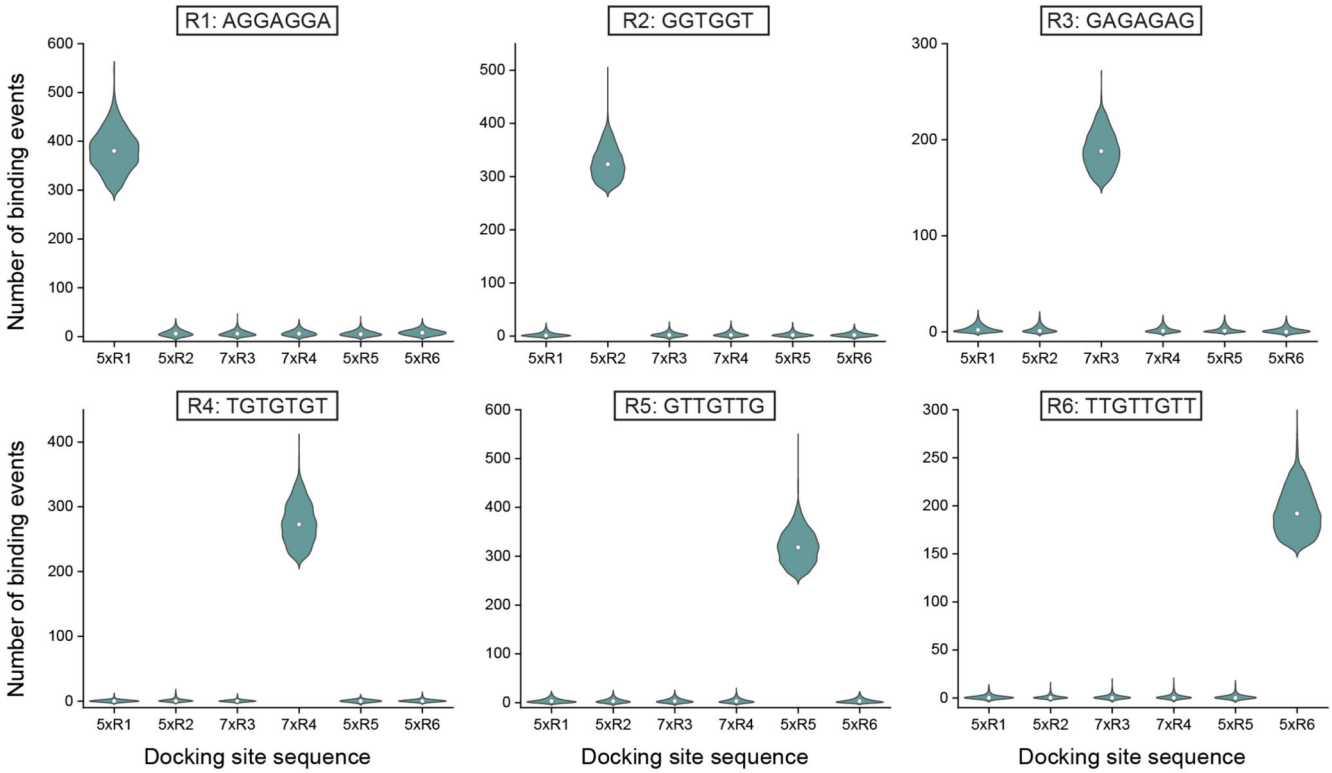

Extended Data Fig. 4.

Europe PMC Funders Author Manuscripts

Europe PMC Funders Author Manuscripts

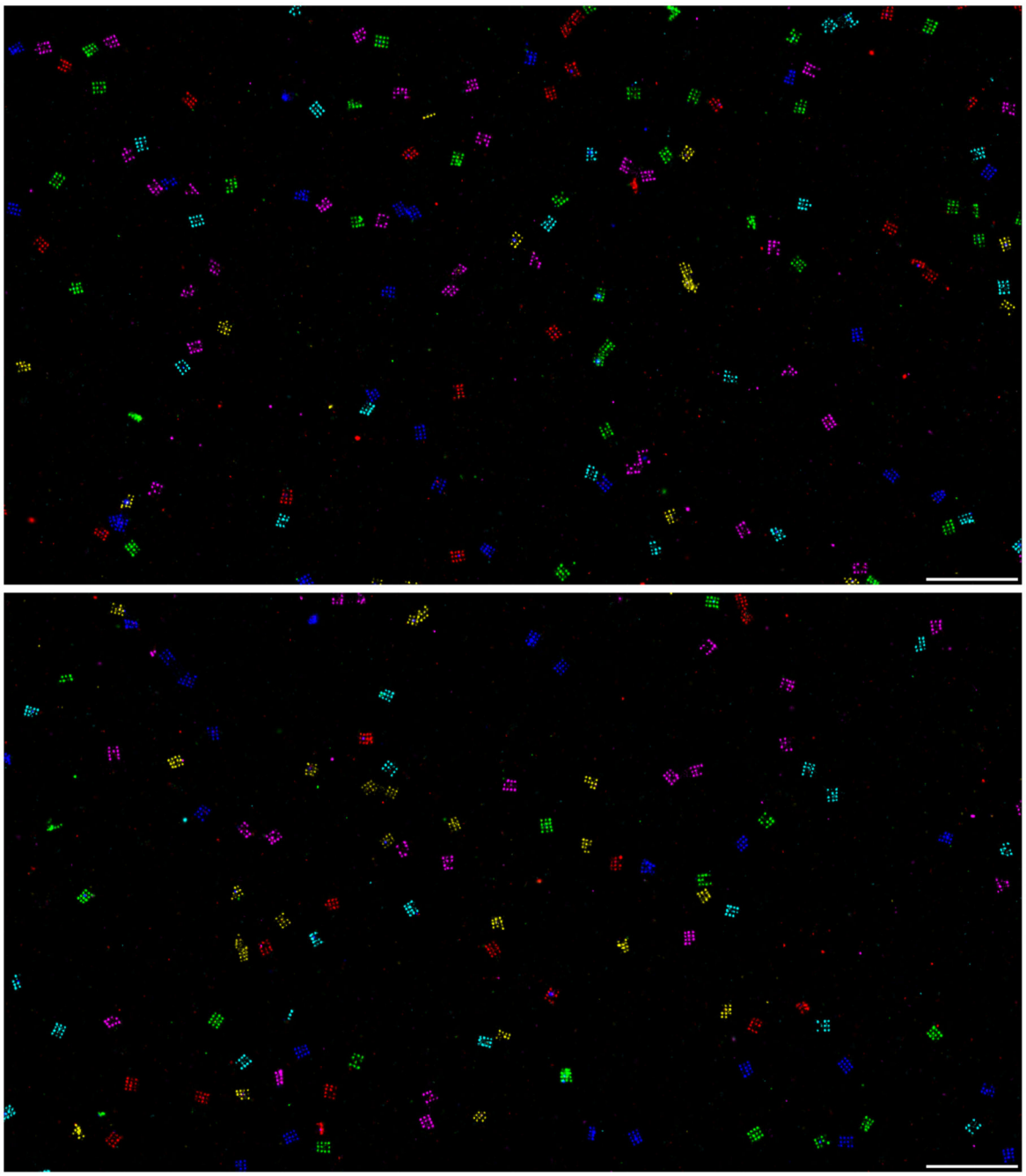

Extended Data Fig. 5.

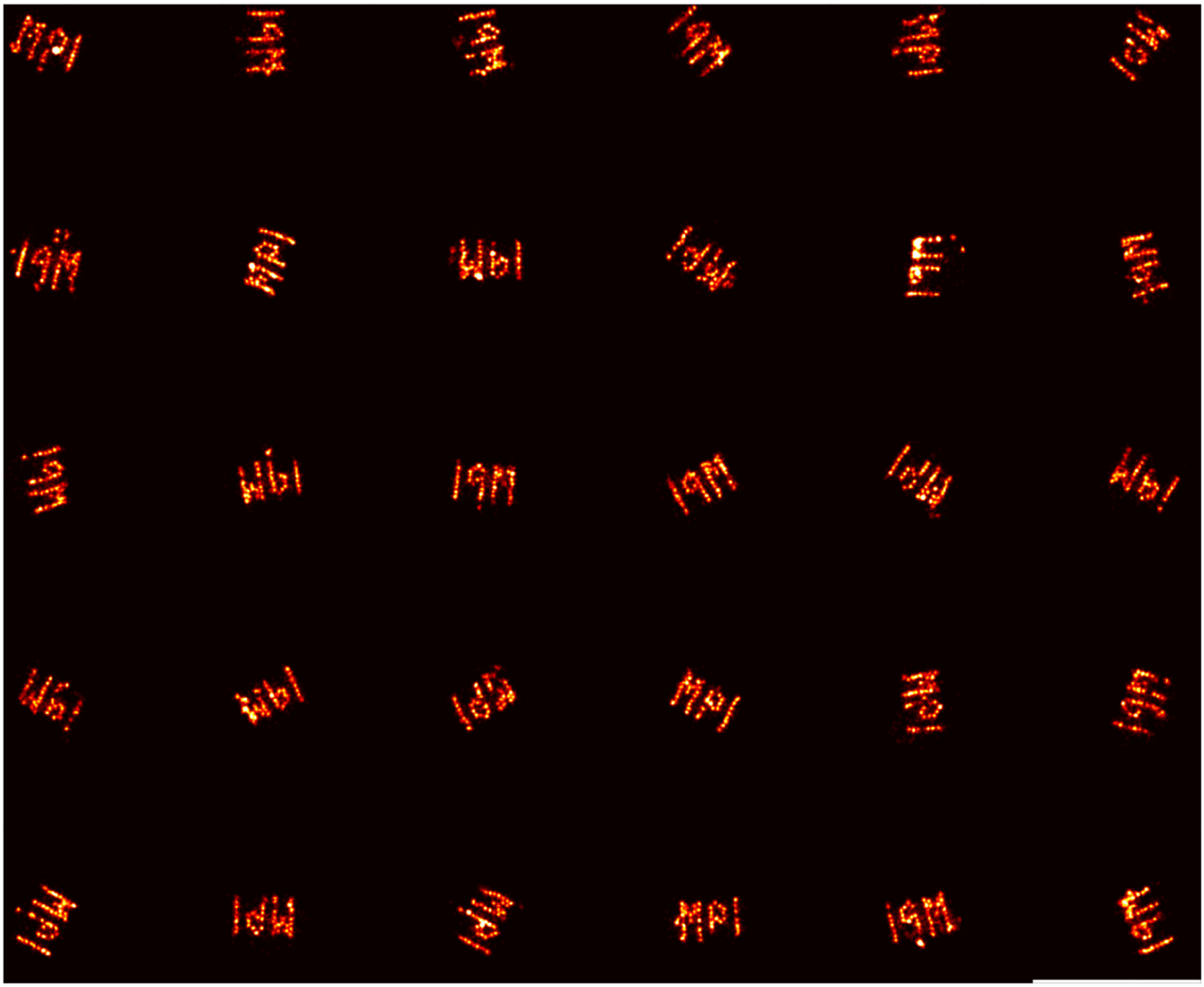

Extended Data Fig. 6.

Europe PMC Funders Author Manuscripts

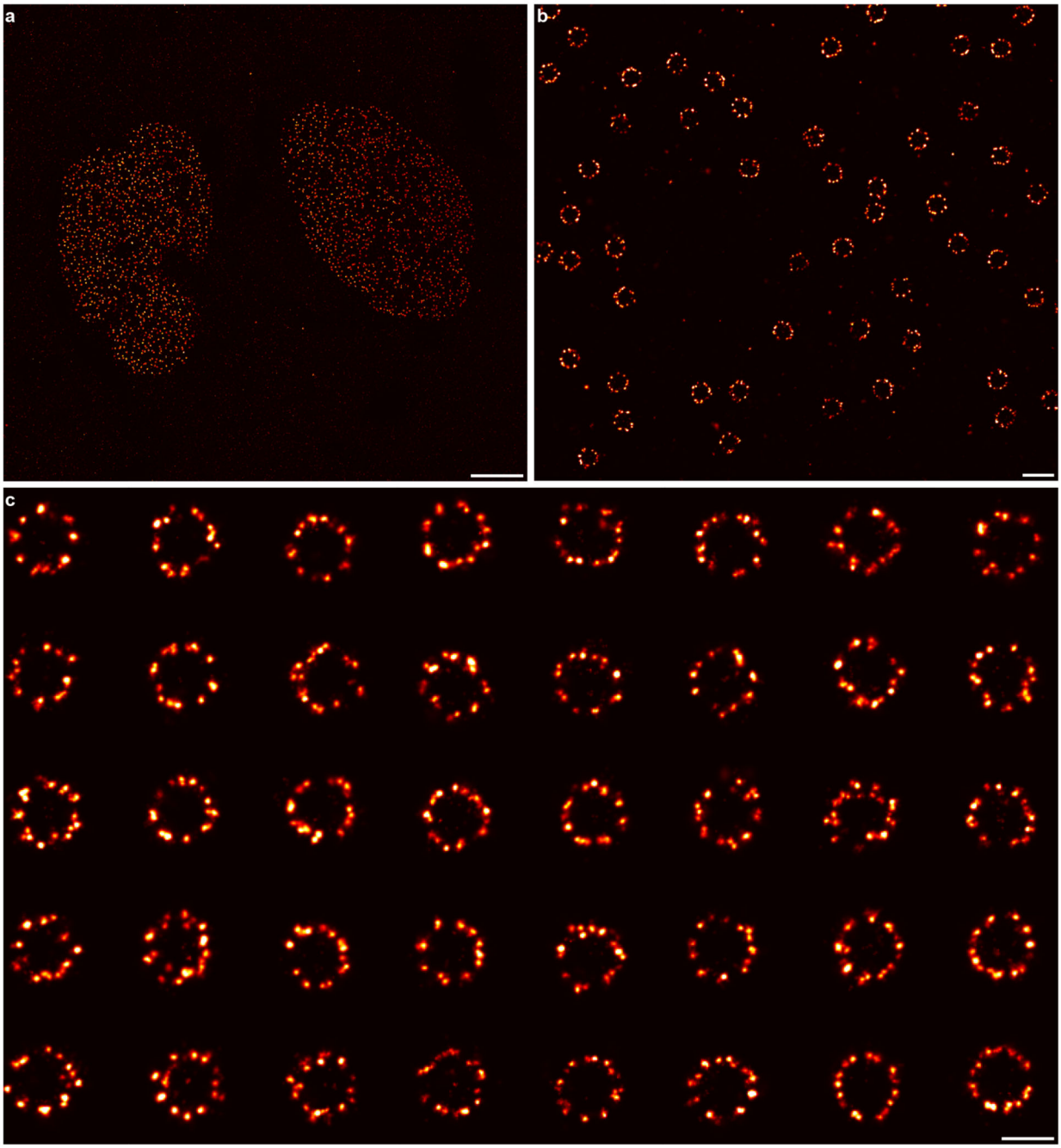

Extended Data Fig. 7.

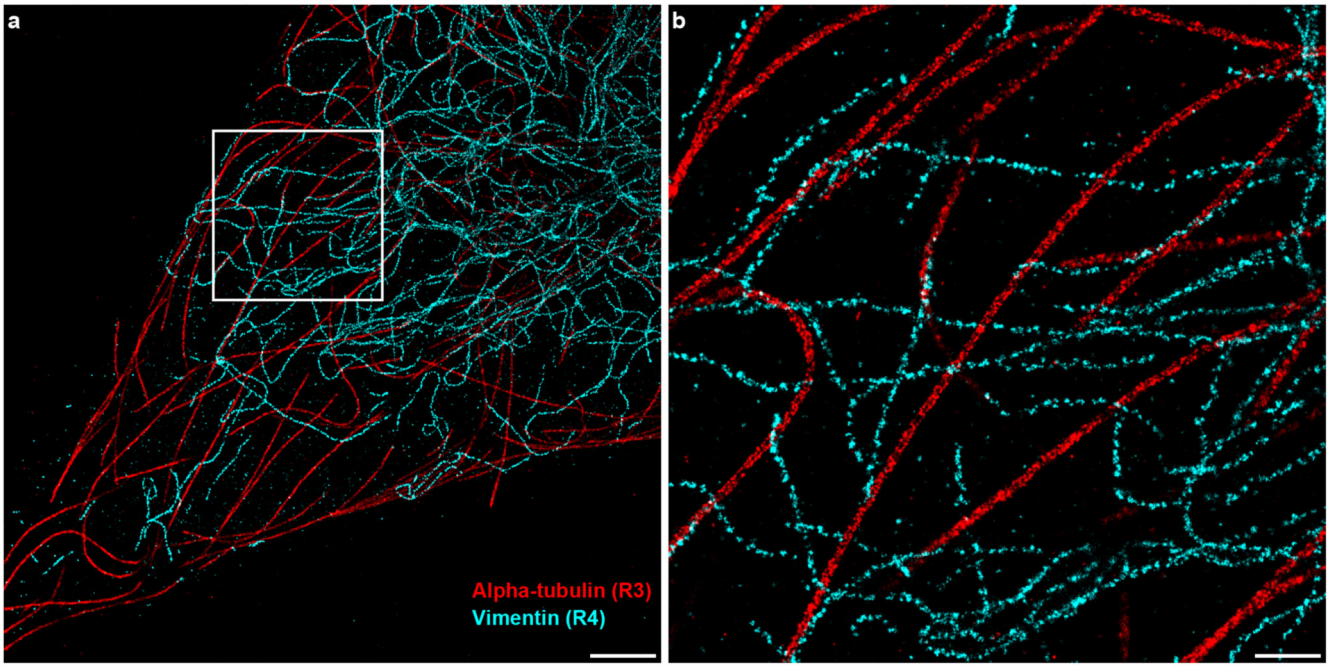

Extended Data Fig. 8.

Europe PMC Funders Author Manuscripts

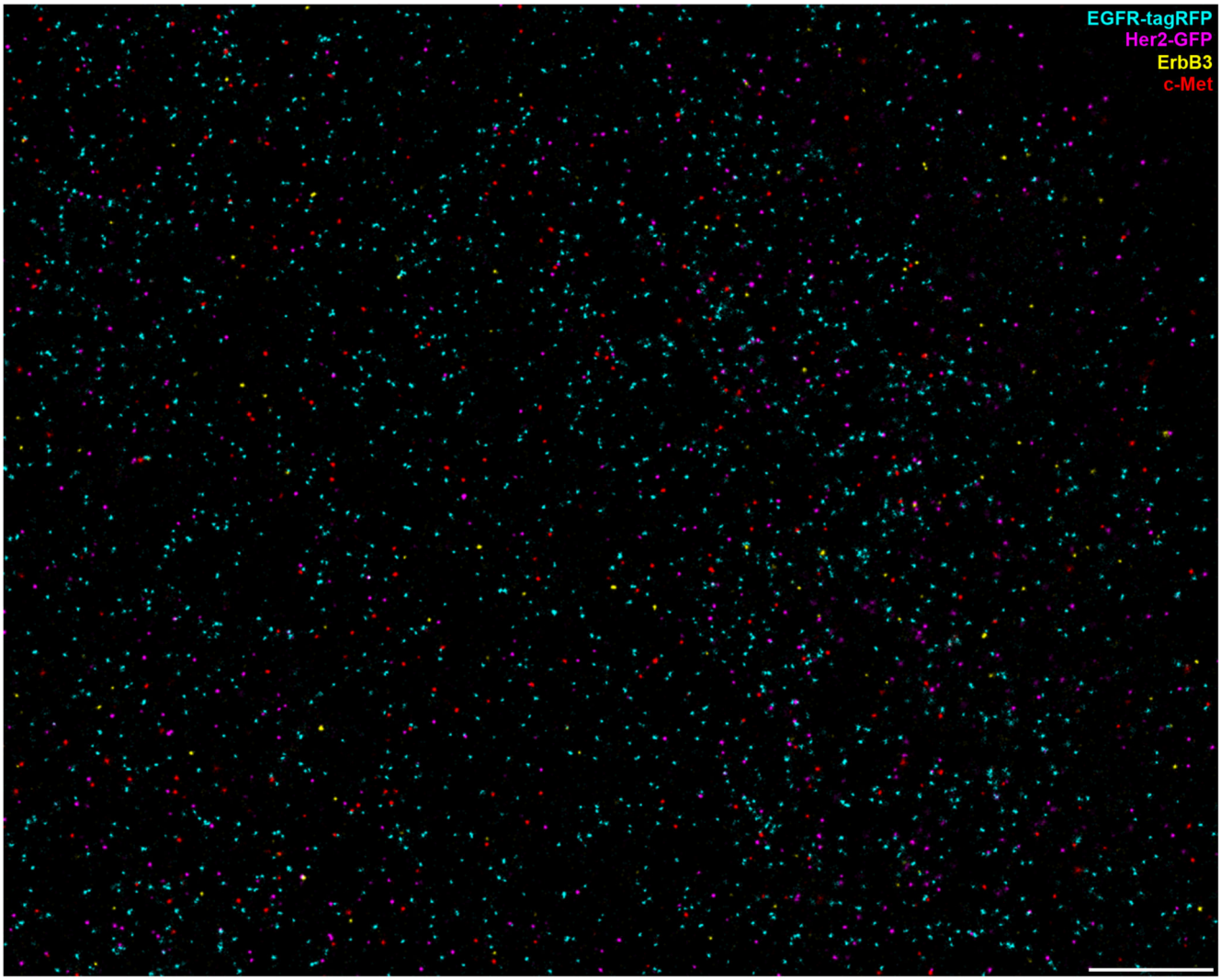

Extended Data Fig. 9.

Europe PMC Funders Author Manuscripts

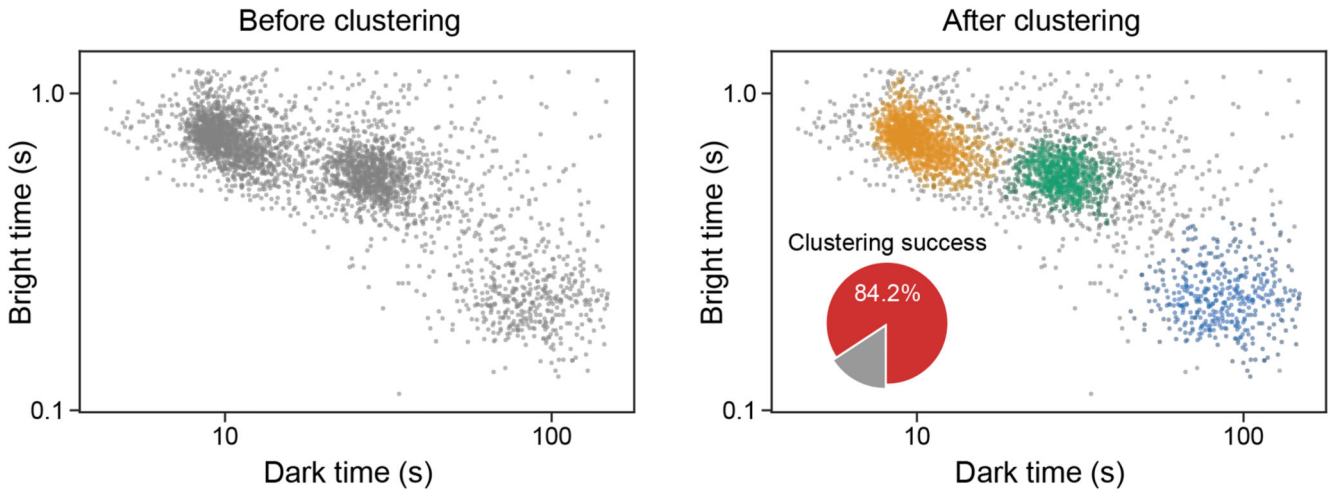

Extended Data Fig. 10.

Supplementary Material

Refer to Web version on PubMed Central for supplementary material.

Acknowledgements

This work has been supported in part by the German Research Foundation through the Emmy Noether Program (DFG JU 2957/1-1), the SFB1032 (project A11), the European Research Council through an ERC Starting Grant (MolMap; grant agreement number 680241), the Allen Distinguished Investigator Program through The Paul G. Allen Frontiers Group, the Max Planck Foundation and the Max Planck Society. We thank the Ries and Ellenberg groups for the kind gift of the Nup96-GFP cell line. We thank Thomas Schlichthaerle, Mahipal Ganji, and Florian Schueder for fruitful discussions. S.S. acknowledges support by the QBM graduate school.

Data availability statement

All raw data is available upon reasonable request from the authors.

References

1. Hell SW, Wichmann J. Breaking the diffraction resolution limit by stimulated emission: stimulated-emission-depletion fluorescence microscopy. Opt Lett. 1994; 19:780–782. [PubMed: 19844443]
2. Betzig E, et al. Imaging intracellular fluorescent proteins at nanometer resolution. Science. 2006; 313:1642–1645. [PubMed: 16902090]
3. Rust MJ, Bates M, Zhuang X. Sub-diffraction-limit imaging by stochastic optical reconstruction microscopy (STORM). Nat Methods. 2006; 3:793–795. [PubMed: 16896339]
4. Schnitzbauer J, Strauss MT, Schlichthaerle T, Schueder F, Jungmann R. Super-resolution microscopy with DNA-PAINT. Nat Protoc. 2017; 12:1198–1228. [PubMed: 28518172]
5. Strauss S, et al. Modified aptamers enable quantitative sub-10-nm cellular DNA-PAINT imaging. Nat Methods. 2018; 15:685–688. [PubMed: 30127504]
6. Schlichthaerle T, et al. Site-Specific Labeling of Affimers for DNA-PAINT Microscopy. Angew Chem Int Ed Engl. 2018; 57:11060–11063. [PubMed: 29873161]
7. Jungmann R, et al. Multiplexed 3D cellular super-resolution imaging with DNA-PAINT and Exchange-PAINT. Nat Methods. 2014; 11:313–318. [PubMed: 24487583]
8. Dai M, Jungmann R, Yin P. Optical imaging of individual biomolecules in densely packed clusters. Nat Nanotechnol. 2016; 11:798–807. [PubMed: 27376244]

9. Schickinger M, Zacharias M, Dietz H. Tethered multifluorophore motion reveals equilibrium transition kinetics of single DNA double helices. Proc Natl Acad Sci U S A. 2018; 115:E7512–E7521. [PubMed: 30037988]
10. Schueder F, et al. An order of magnitude faster DNA-PAINT imaging by optimized sequence design and buffer conditions. Nat Methods. 2019; 16:1101–1104. [PubMed: 31591576]
11. Filius M, et al. High-Speed Super-Resolution Imaging Using Protein-Assisted DNA-PAINT. Nano Lett. 2020
12. Jungmann R, et al. Quantitative super-resolution imaging with qPAINT. Nat Methods. 2016; 13:439–442. [PubMed: 27018580]
13. Rothemund PW. Folding DNA to create nanoscale shapes and patterns. Nature. 2006; 440:297–302. [PubMed: 16541064]
14. Blumhardt P, et al. Photo-Induced Depletion of Binding Sites in DNA-PAINT Microscopy. Molecules. 2018; 23
15. Aitken CE, Marshall RA, Puglisi JD. An oxygen scavenging system for improvement of dye stability in single-molecule fluorescence experiments. Biophysical Journal. 2008; 94:1826–1835. [PubMed: 17921203]
16. Schlichthaerle T, et al. Direct Visualization of Single Nuclear Pore Complex Proteins Using Genetically-Encoded Probes for DNA-PAINT. Angew Chem Int Ed Engl. 2019; 58:13004–13008. [PubMed: 31314157]
17. Pleiner T, et al. Nanobodies: site-specific labeling for super-resolution imaging, rapid epitope-mapping and native protein complex isolation. Elife. 2015; 4:e11349. [PubMed: 26633879]
18. Thevathasan JV, et al. Nuclear pores as versatile reference standards for quantitative superresolution microscopy. Nat Methods. 2019; 16:1045–1053. [PubMed: 31562488]
19. Gwosch KC, et al. MINFLUX nanoscopy delivers 3D multicolor nanometer resolution in cells. Nat Methods. 2020; 17:217–224. [PubMed: 31932776]
20. Sograte-Idrissi S, et al. Nanobody Detection of Standard Fluorescent Proteins Enables Multi-Target DNA-PAINT with High Resolution and Minimal Displacement Errors. Cells. 2019; 8
21. Endesfelder U, Malkusch S, Fricke F, Heilemann M. A simple method to estimate the average localization precision of a single-molecule localization microscopy experiment. Histochem Cell Biol. 2014; 141:629–638. [PubMed: 24522395]
22. Wade OK, et al. 124-Color Super-resolution Imaging by Engineering DNA-PAINT Blinking Kinetics. Nano Lett. 2019; 19:2641–2646. [PubMed: 30864449]
23. Wagenbauer KF, et al. How We Make DNA Origami. Chembiochem. 2017; 18:1873–1885. [PubMed: 28714559]
24. Campello, RJGB, Moulavi, D, Sander, J. Springer Berlin Heidelberg; Berlin, Heidelberg: 2013. 160–172.

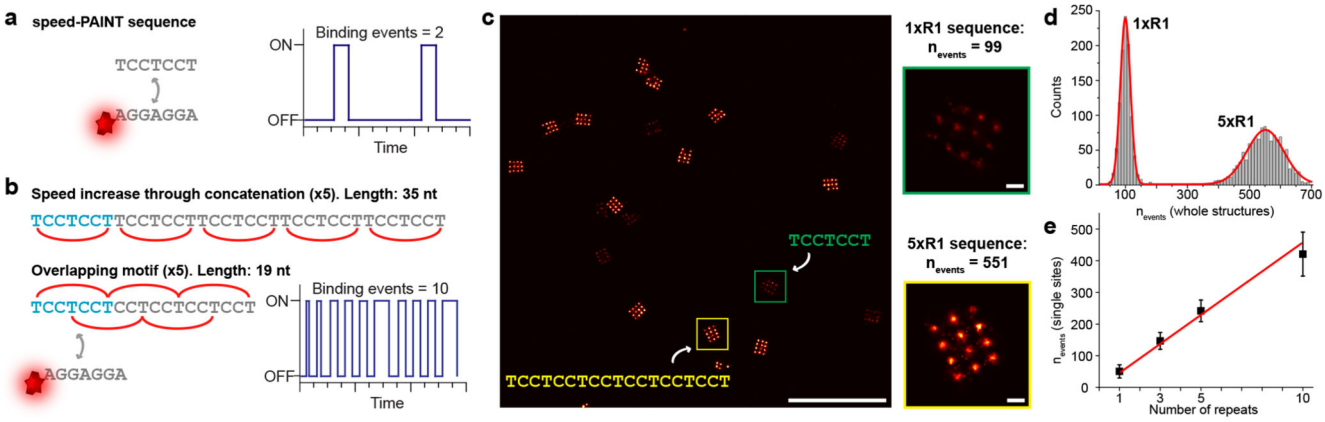

Fig. 1. Faster DNA-PAINT through overlapping sequence motifs.

(**a**) A single speed-optimized DNA-PAINT sequence exhibits a certain number of binding events (e.g. two per unit time). (**b**) Concatenation leads to a linear increase in binding frequency and thus imaging speed (top). However, sequence length increases linearly with the number of binding sites (e.g. from 7 nt for one to 35 nt for five binding sites). Using periodic sequence motifs enables overlapping binding sites, thus allowing shorter docking sequences (e.g. from 7 nt to only 19 nt, while maintaining a 5x speed increase). (**c**) Proof-of-concept using two 20-nm-grid DNA origami carrying 1xR1 and 5xR1 sequence extensions, respectively, shows an increase in the number of binding events (insets: zoom-ins from highlights in the overview, n = 2226). (**d**) Analysis of binding events for whole DNA origami structures from **c** shows an increase in events for the 5xR1 sequence motif (n = 2226). (**e**) Comparing the number of binding events for single docking strands featuring 1x, 3x, 5x, and 10x binding motifs shows a linear increase in the number of binding events (n = 3805). Centers depict the mean value of the Gaussian fit and error bars the standard deviation of the fit. Scale bars, 500 nm (**c**, overview), 20 nm (**c**, zoom-ins). Each experiment was repeated three times independently with similar results.

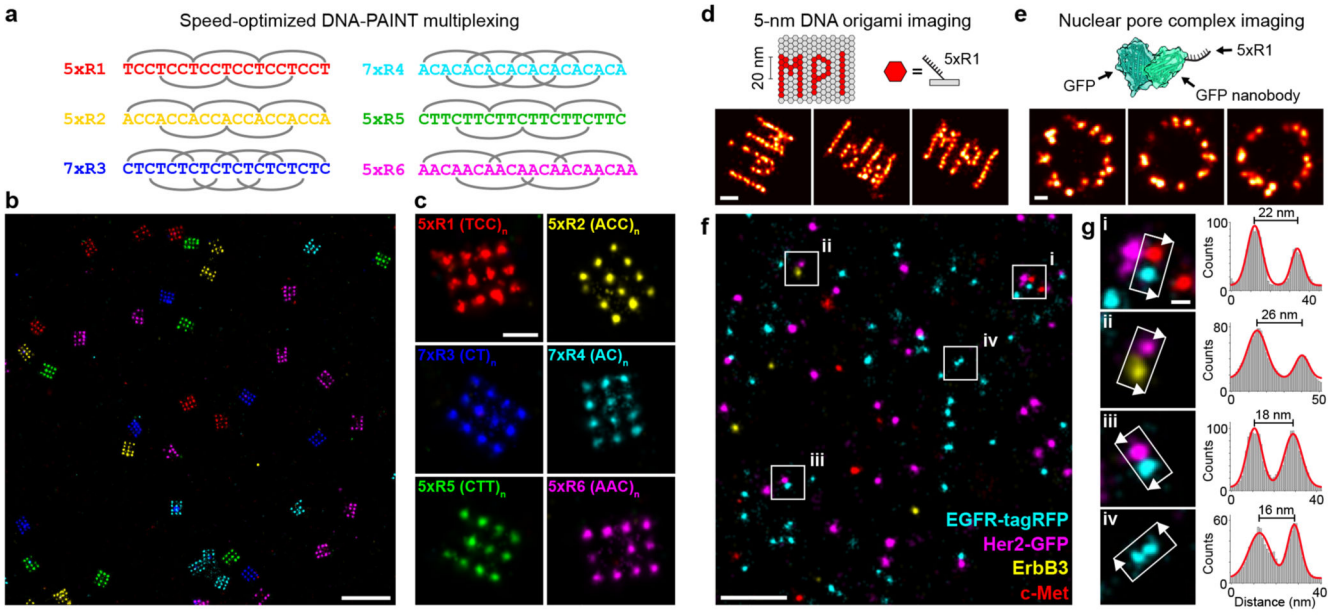

Fig. 2. Multiplexing with concatenated speed-optimized motifs.

(**a**) Designing six orthogonal binding motifs enables speed-optimized multiplexing in Exchange-PAINT experiments. (**b**) Proof-of-concept experiments using 20-nm-grid DNA origami with six orthogonal sequence motifs resolved in 5 minutes per round. (**c**) Exemplary structures from experiment depicted in **b**. (**d**) Imaging of 5-nm-features on 'MPI' origami structures carrying 5xR1 binding sites. 5-nm features are well-resolved, confirming that extending the length of docking sites to 19 nt does not impair spatial resolution. (**e**) EGFP-Nup96 proteins labeled with nanobodies that are site-specifically coupled to 5xR1 docking sites. DNA-PAINT imaging shows specific and efficient labeling of nuclear pore complexes with high quality and spatial resolution. (**f**) Cellular proof-of-concept study using four orthogonal overlapping sequence motifs targeting cell surface receptors (EGFR, Her2, ErbB3, and c-Met) using a combination of DNA-conjugated primary nanobodies (against EGFR-tagRFP and Her2-GFP) and secondary nanobodies against primary antibodies (ErbB3 and c-Met). (**g**) Four-plex Exchange-PAINT with improved docking site sequences enables single-protein resolution, revealing presumably homo- and heterodimers of Receptor Tyrosine Kinases (RTKs), highlighted by c-Met-EGFR- (**i**), Her2-ErbB3- (**ii**), EGFR-Her2-heterodimes, and EGFR homodimers (**iv**) with distances measures between 16 and 26 nm using a cross-sectional histogram analysis. Scale bars, 200 nm (**b**), 40 nm (**c**), 20 nm (**d**, **e**, **g**), and 200 nm (**f**). Each experiment was repeated three times independently with similar results.